Photoefficiency and Optical, Microstructural, and Structural Properties of TiO_2 Thin Films Used as Photoanodes

Francisco Gracia, Juan P. Holgado, and Agustín R. González-Elipe*

Instituto de Ciencia de Materiales de Sevilla (CSIC−University of Sevilla) and Department of Química Inorgánica, Avda. Américo Vespucio s/n, 41092 Sevilla, Spain

Received June 6, 2003. In Final Form: October 24, 2003

The present paper tries to determine, for TiO_2 in the form of thin films, the influence of sample characteristics such as crystallinity and microstructure on photoefficiency. TiO_2 thin films have been prepared by ion beam induced and plasma enhanced chemical vapor deposition at room temperature and 523 K. The thin films have also been annealed at increasing higher temperatures to modify their structural and microstructural characteristics. Depending on the preparation protocol and annealing treatments, thin films have been prepared with different crystallographic structure, texture, and microstructure, as determined by X-ray diffraction and scanning electron microscopy. Nonstoichiometric thin films with a high concentration of Ti^{3+} centers have been also prepared by using an oxygen-poor plasma gas during plasma enhanced chemical vapor deposition. The rutilization behavior of the anatase thin films after annealing at a high temperature has also been investigated. This study has shown that rutilization only starts at 1023 K for the most compact films, while it requires a slightly higher temperature for the more porous thin films. The optical properties of the films have been analyzed by UV−visible absorption spectroscopy and ellipsometry. The photoefficiency of the TiO_2 thin films used as photoanodes has been measured in a photoelectrochemical cell, and the results have been correlated with the different sample characteristics. From this comparison, a clear picture arises, showing that the anatase structure, a high porosity, and a columnar-type growth of the TiO_2 thin films are beneficial factors favoring the photoefficiency of the system.

Introduction

The optical and photocatalytic properties of TiO_2 have been widely studied for more than three decades owing to the large interest that generates from this material being used as optical coating[1,2] or as photocatalytic material for different applications such as, for example, the removal of wastes,[3,4] the photosplitting of water (refs 5 and 6 and references therein), and so forth. Excellent review papers have been published recently with an updated view of the last investigations in this area.[6−9]

The most widely used form of TiO_2 photocatalysts is as a powder material. However, the use of conventional powder catalysts in liquid media is disadvantageous for stirring during the reaction and, once it has been completed, for separation and recovery purposes.[10] This has led to the development of TiO_2 photocatalysts in the form of layers which, among other applications, have been employed as photoanodes in photoelectrochemical cells. TiO_2 photoanodes in photoelectrochemical cells can be grown thermally or electrochemically on Ti foils.[11,12] More recently, TiO_2 thin film photocatalysts have been prepared by different methods including either "wet" (i.e., sol−gel, spray pyrolysis, and related techniques)[13,14] or "dry" procedures (i.e., physical vapor deposition, chemical vapor deposition, and other related techniques).[15−17] Among this latter type of synthesis methods, we must mention the use of plasma enhanced chemical vapor deposition (PECVD), which permits an independent control of the temperature during the deposition of the films.[18,19] From the two methods employed in the present work for the preparation of TiO_2 thin films, this one has furnished the most efficient type of photocatalysts. The possibility to have an effective control of the thickness, structure, and microstructure of the prepared thin films as well as the possibility to synthesize them on any kind of substrates are some of the reasons that have fostered the use of this type of methodology. Another obvious advantage of using thin film technologies for preparing TiO_2 photocatalysts is that typical methods of investigation of thin films can be used to characterize photoanodes.

* Author to whom correspondence should be addressed. E-mail: agustin@cica.es.

(1) Mergel, D.; Buschendorf, D.; Eggert, S.; Grammes, R.; Samset, B. *Thin Solid Films* **2000**, *371*, 218.
(2) Leprince-Wang, Y.; Yu-Zhang, K.; Nguyen Van, N.; Souche, D.; Rivory, J. *Thin Solid Films* **1997**, *307*, 38.
(3) Ollis, D. F., Al-Ekabi, H., Eds. *Photocatalytic Purification and Treatment of Water and Air*; Elsevier: Amsterdam, 1993.
(4) Cermenati, L.; Pichat, P.; Guillard, Ch.; Albini, A. *J. Phys. Chem. B* **1997**, *101*, 2650.
(5) Uchida, H.; Katoh, Sh.; Watanabe, M. *Electrochim. Acta* **1998**, *93*, 2111.
(6) Back, T.; Nowotny, J.; Rekas, M.; Soreell, C. C. *Int. J. Hydrogen Energy* **2002**, *27*, 991.
(7) Hagfeldt, A.; Grätzel, M. *Chem. Rev.* **1995**, *95*, 49.
(8) Linsebigler, A. L.; Lu, G.; Yates, J. T., Jr. *Chem. Rev.* **1995**, *95*, 735.
(9) Herrmann, J. M. *Catal. Today* **1995**, *24*, 157.
(10) Wang, C.; Wang, T.; Zheng, Sh. *Physica E* **2002**, *14*, 242.
(11) Kavan, L.; Oregan, B.; Kay, A.; Grätzel, M. *J. Electroanal. Chem.* **1993**, *346*, 291.
(12) Natarajan, C.; Nogami, G. *J. Electrochem. Soc.* **1996**, *143*, 1547.
(13) Chrysicopoulou, P.; Davazoglon, D.; Trapalis, Ch.; Korda, G. *Thin Solid Films* **1998**, *323*, 188.
(14) Natarajan, C.; Fukunaga, N.; Nogami, G. *Thin Solid Films* **1998**, *322*, 6.
(15) Okimura, K. *Surf. Coat. Technol.* **2001**, *135*, 286.
(16) Battiston, G. A.; Gerbasi, R.; Porchia, M.; Rizzo, L. *Adv. Mater. CVD* **1999**, *5*, 73.
(17) Ding, X.-Z.; Zhang, F.-M.; Wang, H.-M.; Chen, L.-Z.; Liu, X.-H. *Thin Solid Films* **2000**, *368*, 257.
(18) Battiston, G. A.; Gerbasi, R.; Gregori, A.; Porchia, M.; Cattarin, S.; Rizzi, G. A. *Thin Solid Films* **2000**, *371*, 126.
(19) da Cruz, N. C.; Rangel, E. C.; Wang, J.; Trasferetti, B. C.; Davanzo, C. V.; Castro, S. G. C.; de Moraes, M. S. B. *Surf. Coat. Technol.* **2000**, *126*, 123.

10.1021/la034998y CCC: $27.50
Published on Web 02/06/2004

Systematic studies with TiO_2 powder photocatalysts have permitted the establishment of correlations between photoactivity and sample parameters such as the structure, particle size, surface area, and so forth.[20−22] By contrast, and despite the significant effort done during the last years to study thin film photocatalysts, the information about the influence of certain characteristics of the thin films such as structure, microstructure, optical properties, and so forth on their efficiency as photoanodes is still rather scarce. An example of this type of study is the paper of Takahashi et al.[23] where these authors show an inverse dependence between the thickness of the film and the photoefficiency. However, the variation with thickness and, therefore, the dependence of the measured photoactivity of other sample characteristics such as porosity, crystallinity, and so forth were not addressed in that paper.

With the present work, we want to improve the understanding of the factors that control the photoefficiency of TiO_2 thin films. For this purpose, two series of different TiO_2 thin films have been prepared by ion beam induced chemical vapor deposition (IBICVD) and PECVD under different deposition conditions. These two methods have been chosen because, in principle, the first one yields very compact thin films,[24] while the second one, particularly when deposition is carried out at a low temperature, may produce films with a higher porosity.[25] The obtained films have been carefully characterized by different techniques, and the obtained structural and microstructural data correlated with their optical properties (refractive index and absorption coefficient) and photoresponse as determined in a photoelectrochemical cell. The following sample characteristics have been considered for this study: crystallographic structure and texture, microstructure, and degree of nonstoichiometry. Another point that has been also addressed in the paper is the dependence on the temperature of the anatase/rutile transformation. Although in bulk and powder forms this transformation occurs around 873−973 K,[26] in the case of small particles and thin films the transformation seems to occur at higher temperature and depends on sample characteristics.[18,27−30] The study carried out here for TiO_2 thin films has revealed a similar tendency of phase transformation toward higher temperatures but also a certain dependence on thin film compactness.

Experimental Details

TiO_2 thin films have been prepared by PECVD and IBICVD. The temperature of the substrate during deposition was controlled from room temperature up to 623 K. The PECVD thin films were prepared in a plasma reactor with a "downstream" configuration and an external microwave ECR source (SLAN) operated at 400 W.[25] The plasma source was supplied with O_2 or mixtures of O_2 + Ar (this latter condition has been intented for the synthesis of nonstoiochiometric thin films). Ti-*iso*-$(OC_3H_7)_4$ was used as precursor of Ti. Because at room temperature the vapor pressure of this compound is too low, to dose it directly into the chamber, it was heated at 313 K while O_2 (5 sscm) was flowing through it. Both the conducting line and a shower-type dispenser placed in the deposition chamber were heated at 373 K to prevent condensation of the precursor. Under the previous conditions, a growing rate of approximately 4 nm min^{-1} was measured for the films prepared with the substrate at room temperature. An increase of the growth rate was determined for higher temperatures.

The IBICVD procedure consists of the decomposition of a metal volatile precursor under the action of a beam of accelerated O_2^+ ions. A more detailed description of this procedure can be found in ref 31. For the synthesis of TiO_2 thin films, 4×10^{-5} Torr of $TiCl_4$ were dosed over a turnable substrate holder that was bombarded with a beam of O_2^+ ions of 400 eV kinetic energy and a current density of ∼120 μA cm^{-2}. The ion source used was a RF (radio frequency) operated ion gun that was supplied with O_2 at a partial pressure of 5×10^{-4} Torr measured in the deposition chamber.

For both PECVD and IBICVD, deposition was done simultaneously on different substrate materials as required for specific tests or applications. Si(100) substrates were used for scanning electron microscopy (SEM), fourier transform infrared spectroscopy, X-ray diffraction (XRD), and ellipsometry analysis, quartz plates for ultraviolet−visible spectroscopy (UV−vis) analysis, and titanium metal foils for electrochemical tests. Thin films were prepared with the substrate either at room or at higher temperatures. Samples prepared at room temperature were eventually annealed in air for 3 h at a high temperature. To discern the different thin film samples studied here, we will use the following notation trough the text: (P, I)TiO_2-$T_1(T_2)$, where P or I mean samples prepared by PECVD or IBICVD, T_1 is the temperature during preparation and T_2 that of annealing. This second temperature, always written in parentheses, is omitted if the sample is not annealed after preparation. When the PECVD samples are prepared with mixtures of Ar + O_2 as plasma gas, the used notation reads as (P−*N*Ar)TiO_2-$T_1(T_2)$, where *N* refers to the percentage of Ar in the plasma gas.

The thickness of the films was between 0.4 and 1 μm, a range where the dependence between the thickness and photoefficiency has not been observed.[23] The sample microstructure was determined by SEM in a JEOL JSM-5400 instrument. Optical properties of the films were determined by UV−vis absorption spectroscopy and, for some selected samples, by spectroscopic ellipsometry. For the first type of studies, the thin films, deposited on quartz plates, were analyzed in the transmission mode in a Shimadzu 2101 spectrometer. The spectroscopic ellipsometer experiments were performed using a SOPRA commercially available system. The measurements of ellipsometric parameters were made at wavelengths from 0.21 to 1.0 μm at different angles of incidence. The analysis procedure consists of a regression using a Cauchy law to simulate the refraction index $n(\lambda)$ and to extract the absorption coefficient $k(\lambda)$ of the layer. Reported refraction index values determined by UV−vis or ellipsometry were determined at $\lambda = 550$ nm.

The structure of the films was analyzed by XRD in a Siemens D5000 instrument with the Bragg−Brentano configuration. Texture coefficients of crystal planes were determined by the typical formulas yielding information on preferential growth.[32] The sizes of the crystalline domains were determined with the formula of Scherrer.

Measurement of the photoelectrochemical response of samples was done by irradiating a 1-cm^2 area of a TiO_2 thin film deposited on a Ti foil that was immersed in a KCl (0.5 M) + $Na_2C_2O_4$ (5×10^{-3} M) solution bubbled with N_2. Unmonochromatized light emitted by a 125-W Xe lamp (Cermax) was used for the irradiation. Photocurrent measurements were done in a photoelectrochemcial cell with respect to the difference of voltages between the photoanode (i.e., TiO_2) and a calomelane reference

(20) Arada, H.; Ueda, T. *Chem. Phys. Lett.* **1984**, *106*, 229.
(21) Montoya, I. A.; Viveros, T.; Domínguez, J. M.; Canales, L. A.; Schifter, I. *Catal. Lett.* **1992**, *15*, 207.
(22) Degan, G.; Tomkiewicz, M. *J. Phys. Chem.* **1993**, *97*, 12651.
(23) Takahashi, M.; Tsukigi, K.; Uchino, T.; Yoko, T. *Thin Solid Films* **2001**, *388*, 231.
(24) González-Elipe, A. R.; Yubero, F.; Sanz, J. M. *Low Energy Ion Assisted Film Growth*; Imperial College Press: Singapore, 2003.
(25) Barranco, A.; Yubero, F.; Cotrino, J.; Espinós, J. P.; Benítez, J.; Rojas, T. C.; Allain, J.; Girardeau, T.; Riviere, J. P.; González-Elipe, A. R. *Thin Solid Films*; **2001**, *396*, 9.
(26) Lobl, P.; Huppertz, M.; Mergel, D. *Thin Solid Films* **1994**, *251*, 72.
(27) Martin, N.; Rousselot, Ch.; Rondot, D.; Palmino, F.; Mercier, R. *Thin Solid Films* **1997**, *300*, 113.
(28) Martin, N.; Rousseau, Ch. *Thin Solid Films* **2000**, *377*, 550.
(29) Ragai, J.; Lotfi, W. *Colloids Surf.* **1991**, *61*, 97.
(30) Criado, J. M.; Real, C. *Trans. Faraday Soc.* **1983**, *179*, 2765.
(31) Espinós, J. P.; Caballero, A.; Jiménez, V. M.; Sánchez-López, J. C.; Contreras, L.; Leinen, D.; González-Elipe, A. R. *Adv. Mater. CVD* **1997**, *3*, 219.
(32) Jiménez, V. M.; Espinós, J. P.; Caballero, A.; Contreras, L.; Fernández, A.; Justo, A.; González-Elipe, A. R. *Thin Solid Films* **1999**, *353*, 113.

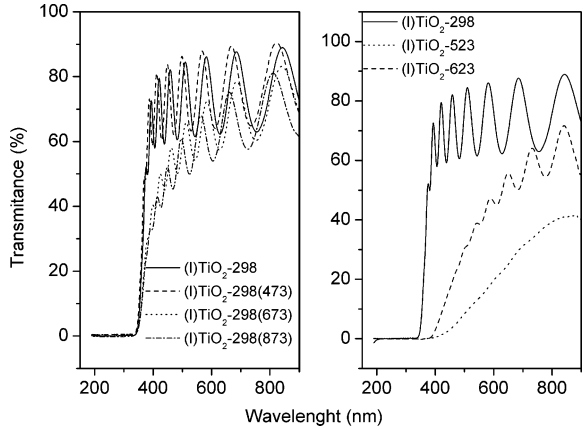

Figure 1. UV−vis absorption spectra of the indicated TiO_2 thin films: (left) samples prepared by IBICVD at room temperature and then annealed at the indicated temperatures; (right) samples prepared by IBICVD at the indicated temperatures.

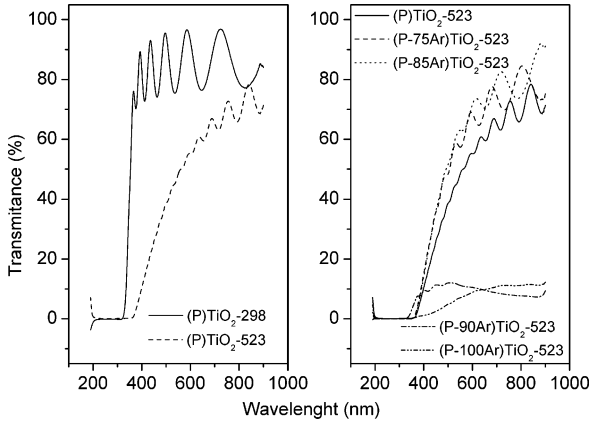

Figure 2. UV−vis absorption spectra of the indicated TiO_2 thin films: (left) samples prepared by PECVD at room temperature and 523 K; (right) samples prepared by PECVD at 523 K with increasing amounts of Ar in the plasma gas.

electrode. The setup of the photoelectrochemical cell was similar to that of Byrne and Eggins.[33] The cathode compartment consisted of a Pt foil immersed in a KCl (0.5 M) solution bubbled with O_2. As a reference for the photoelectrochemical measurements, a photoanode made of anatase Degussa P25 was used. This electrode was prepared by electrophoretic deposition of titania onto a Ti foil[34,35] from a liquid suspension of anatase P25 powders. The foil with deposited powders was then annealed at 673 K for 3 h. To select the visible portion of light emitted from the lamp, for some experiments a polymer plate was used as an UV filter (cutoff $\lambda < 400$ nm).

Results

UV−Vis Absorption of Light. The optical properties of the different TiO_2 samples were first investigated by UV−vis absorption spectroscopy. The left-hand side of Figure 1 shows spectra corresponding to an IBICVD sample prepared at room temperature that has been later annealed in air at increasing higher temperatures up to 873 K [i.e., (I)TiO_2-298(473)(673)(873)]. These spectra are characterized by the well-known oscillations appearing when a transparent thin film of a material of high refractive index is deposited on a lower refractive index substrate.[36] From this interference pattern, it is possible to estimate both the thickness and the refractive index of the film. From the spectrum of the (I)TiO_2-298 sample, we deduced a thickness of 700 nm and a refractive index of 2.3. Annealing of the film in air at 673 or 873 K produces a degradation of the quality of the interference pattern (loss of the intensity of the interference bands) that can be interpreted in terms of light scattering at the large well-crystallized domains developed in these samples or into large pores formed after annealing[18,27,28] (see next sections for the crystallization behavior and microstructure of these samples). It is important to stress that the loss of transmittance in the range 350−600 nm in these annealed films is not due to absorption but to the random scattering of light.

The right-hand side of Figure 1 shows a series of spectra of IBICVD TiO_2 thin films prepared with the substrate holder at room temperature, 623, and 523 K. It is interesting that, while samples (I)TiO_2-298 and (I)TiO_2-523 were amorphous, (I)TiO_2-623 was crystalline (see next section). In a similar way as with the previously discussed samples, we attribute the degradation of the interference pattern observed for the (I)TiO_2-523 and (I)TiO_2-623 samples to light scattering by well-crystallized particles formed in the films.

Optical characterization experiments were also carried out with TiO_2 thin films prepared by PECVD. However, in this case the spectra of the TiO_2 thin films prepared at room temperature and then annealed at a high temperature will not be shown because this thermal treatment produces a partial delamination of the film when the substrate was quartz. The spectra shown in the left-hand side of Figure 2 corresponds to samples (P)TiO_2-298 and (P)TiO_2-523. This latter sample was crystalline (see next section for the X-ray characterization of samples), and the degradation of the interference pattern and the enhanced loss of transmittance observed in this case are also attributed to light scattering. From the spectrum of the sample prepared at room temperature, we estimated a thickness of 400 nm and a refraction index of 2.05 for that thin film.

In the right-hand side of Figure 2, we compare spectra of TiO_2 thin films prepared at 523 K with the plasma gas progressively enriched in Ar with the aim of producing nonstoichiometric TiO_2 thin films. The spectra of samples prepared with 75 and 85% Ar are quite similar (except for the number of oscillations that indicate a slightly different thickness for the two samples) to that prepared with O_2 as the plasma gas. By contrast, the transmittance of the sample prepared with 90% Ar is quite low in the whole range of analyzed wavelengths. These four samples were crystalline, but were completely different by eye inspection. The three first samples were partially transparent and had a milky aspect when examined at the grazing angle. However, the sample prepared with 90% Ar had a deep blue color, which is indicative of a high degree of nonstoichiometry. It is worth mentioning that, when this sample was examined by Rutherford backscattering spectroscopy (RBS) or X-ray photoelectron spectroscopy (XPS) plus Ar^+ sputtering to clean the surface, no significantly large amounts of C were detected that could account for its dark aspect. On the other hand, the sample prepared with no oxygen in the plasma depicts an even higher absorption and had a deep gray color. It will be shown in the following that it presented no XRD signals and had no photoactivity. The composition of this film was a mixture of titanium oxide plus carbon, as determined by XPS and RBS.

(33) Byrne, J. A.; Eggins, B. R. J. Electroanal. Chem. **1998**, *457*, 61.
(34) Fernández, A.; Lassaletta, G.; Jiménez, V. M.; Justo, A.; González-Elipe, A. R.; Herrmann, J. M.; Tahiri, H.; Ait-Ichon, Y. *Appl. Catal. B* **1995**, *7*, 49.
(35) Byrne, J. A.; Eggins, B. R.; Brown, N. M. D.; Mckinney, B.; Rouse, M. *Appl. Catal., B* **1998**, *17*, 25.
(36) Swanepoel, R. *J. Phys. E* **1983**, *16*, 1213.

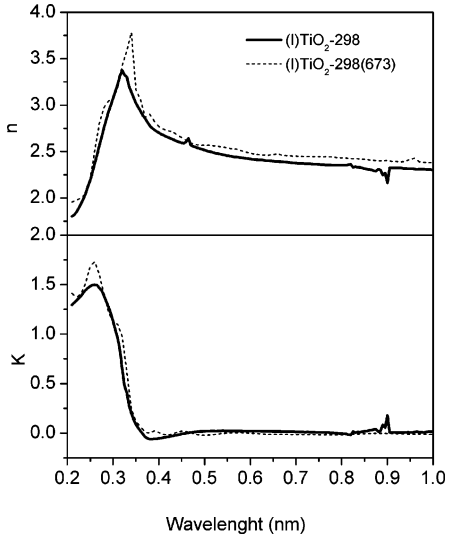

Figure 3. Plots of the *n* and *k* functions against the wavelength determined by ellipsometry for the (I)TiO_2-298 and (I)TiO_2-298(673) samples.

Table 1. Apparent Absorption Thresholds[a] of TiO_2 Thin Films and Values of the Refractive Index for Selected Samples

sample	n (λ = 550 nm) (ellipsometry)	n (λ = 550 nm) (UV−vis)	E_g (eV) (UV−vis)
(I)TiO_2-298	2.456	2.30	3.20
(I)TiO_2-523			1.80
(I)TiO_2-623			2.90
(I)TiO_2-298(673)	2.539	2.35	3.10
(P)TiO_2-298	2.09	2.05	3.30
(P)TiO_2-523			2.90
(P)TiO_2-298(623)	2.00	2.00	3.10
(P-75Ar)TiO_2-523			2.70
(P-85Ar)TiO_2-523			2.90
(P-90Ar)TiO_2-523			3.00

[a] Apparent absorption thresholds have been determined by extrapolation to zero of the $A(h\nu)^{1/2}$ versus $h\nu$ function.[37]

Optical characterization of selected TiO_2 thin films prepared at room temperature and then annealed at 673 K was also done by ellipsometry for samples deposited on Si(100) substrates (on this substrate the PECVD samples did not delaminate upon annealing).

A typical example of the evolution of the *n* and *k* functions with respect to the wavelength of light is shown in Figure 3 for samples prepared by IBICVD. Values of the refractive index at 550 nm are collected in Table 1, where they are compared with those determined by UV−vis absorption for different samples. This table also reports the values of the absorption thresholds estimated from the UV−vis spectra by extrapolation to 0, the edge of the function $A(h\nu)^{1/2}$, represented against $h\nu$.[37] The reported values significantly vary according to the thermal treatments of the samples.

When comparing the different values of the refractive index collected in Table 1, it is apparent that the value of *n* is always higher for the IBICVD films, in agreement with the expected higher density and compactness of thin films prepared under ion irradiation.[24]

Microstructure of TiO_2 Thin Films. The microstructure of TiO_2 thin films is critical for both their optical properties and their photocatalytic behavior. Therefore, a close examination of the microstructure has been carried out by SEM for samples prepared according to different protocols. Figures 4−6 show a series of normal and cross-sectional views of thin films prepared by IBICVD and PECVD under different conditions. The (I)TiO_2-298 thin film is compact and homogeneous with practically no porosity. On the other hand, the (I)TiO_2-523 or (I)TiO_2-623 thin films depict images where well-defined and highly packed crystals can be observed, indicating that although some surface roughness has developed, the films are still rather compact.

In general, the PECVD samples are less compact than those prepared under ion assistance (cf., Figures 5 and 6). The (P)TiO_2-298 sample does not show well-defined structures, although it is more heterogeneous than its equivalent counterpart prepared by IBICVD (cf., Figure 4, left). Annealing of this sample at 623 K [i.e., sample (P)TiO_2-298(623)] leads to the formation of cracks and the development of well-defined agglomerates in the form of columns (cf., Figure 5, middle). It is, therefore, likely that the original films have a considerable microporosity that is not easily detectable by SEM and tends to collapse upon annealing.

By contrast, the (P)TiO_2-523 sample depicts a rather open microstructure where small particles aggregate to form columns with voids and pores between them (see the normal and cross-sectional images of these samples). Well-defined columnar and highly porous microstructures also develop for the PECVD samples prepared at 523 K with mixtures of O_2 + Ar. For this series of thin films, the addition of Ar to the plasma gas seems to favor the formation of well-defined and thin columns.

Crystalline Structure. The crystalline structure of the different TiO_2 thin films was analyzed by XRD. Figure 7 shows XRD diagrams of IBICVD and PECVD samples. The (I)-TiO_2-298 and (I)-TiO_2-523 thin films (for simplicity, the curve of this latter sample is not included in the figure) were amorphous and crystallized into anatase upon annealing at 673 K. The (I)-TiO_2-623 sample also depicted this structure, although the XRD peaks were broader, indicating a poor crystallinity. The size of the crystal domains in the different samples was estimated by means of the Scherrer formula applied to the (101) diffraction peak.

A summary of the crystal sizes is presented in Table 2.

On the other hand, Figure 7 also shows that the (P)TiO_2-298 sample was amorphous and crystallized into the anatase structure upon annealing at 623 K. The (P)TiO_2-523 sample was also characterized by this structure. Figure 7 also shows the diagrams of the samples prepared by PECVD at 523 K with mixtures of O_2 + Ar as the plasma gas. Unlike the (P-100Ar)TiO_2-523 sample, the other thin films were crystalline and presented the anatase structure. The different relative intensity of the diffraction peaks as compared with that of the other samples indicates the development of a preferential texture (i.e., preferential growth of the crystalline planes parallel to the thin film surface). Textural coefficients (T) can be determined according to the formula:[32]

$$T(hkl) = [I(hkl)/I_0(hkl)]/\{(1/n)\sum[I(hkl)/I_0(hkl)]\}$$

where $I(hkl)$ are the intensitities of the (hkl) diffraction peaks in the samples and $I_0(hkl)$ are the intensities of a reference polycrystalline material with a random orientation of their planes.

The obtained values are presented in Figure 8. A first assessment of this figure indicates that the IBICVD samples present either a preferential growth of the (101) planes [i.e., (I)TiO_2-623 samples] or a slight texturing

(37) Serpone, N.; Lawless, D.; Khairutdinov, R. *J. Phys. Chem.* **1995**, *99*, 16646.

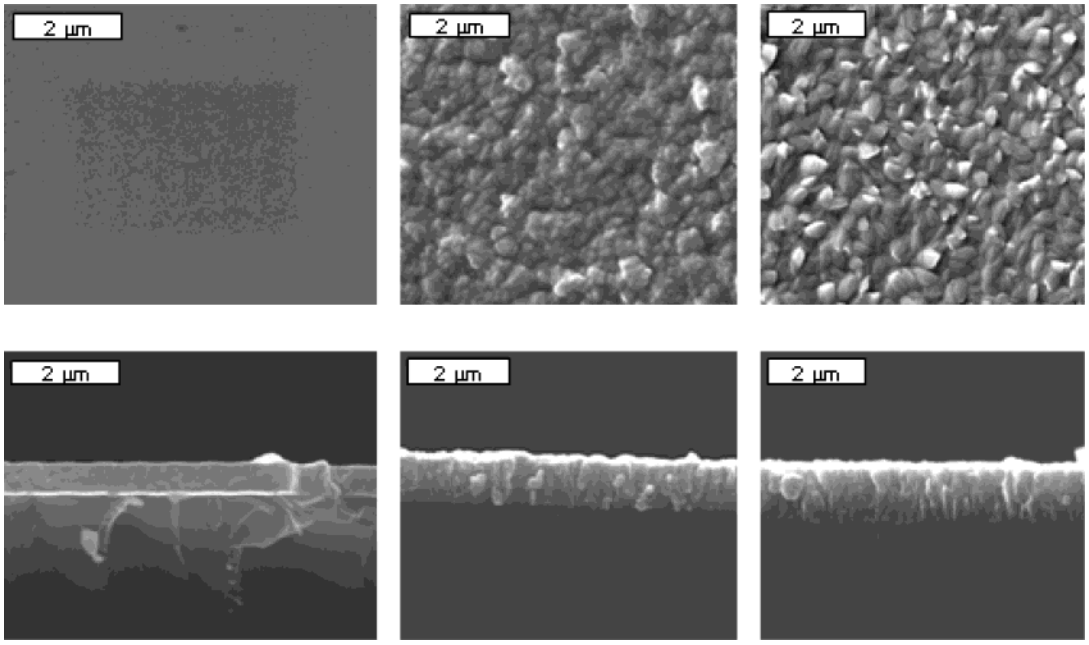

Figure 4. Normal and cross-sectional SEM images of TiO_2 thin films prepared by IBICVD: (left) (I)TiO_2-298; (middle) (I)TiO_2-523; (right) (I)TiO_2-623.

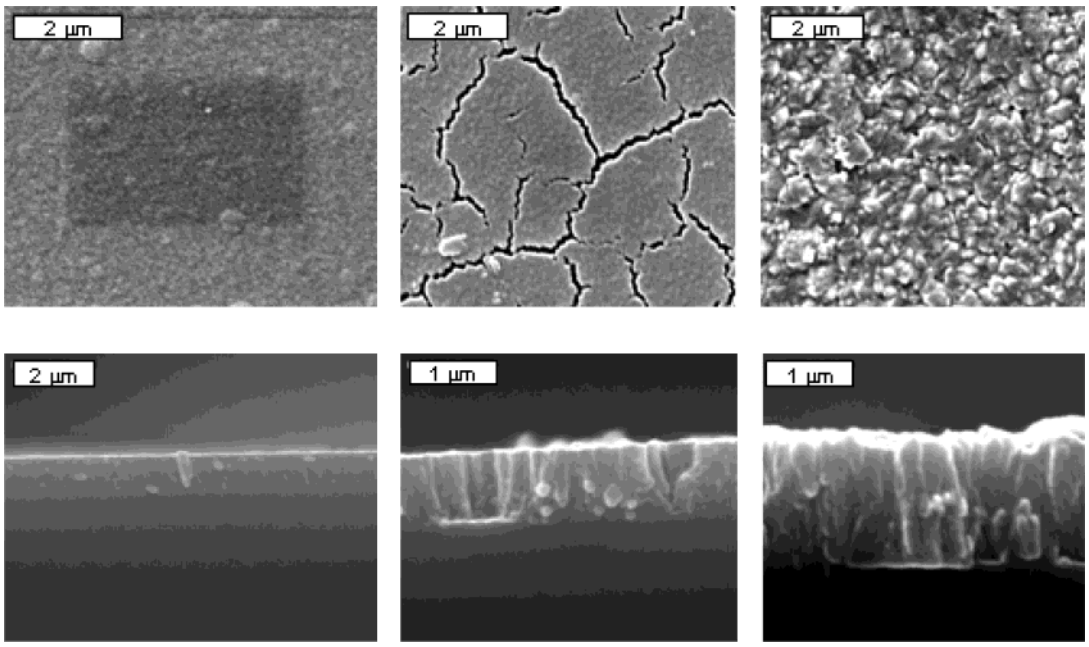

Figure 5. Normal and cross-sectional SEM images of TiO_2 thin films prepared by PECVD: (left) (P)TiO_2-298; (middle) (P)TiO_2-298(623); (right) (P)TiO_2-523.

according to the [200] direction [e.g., (I)TiO_2-298(673) samples]. In contrast, the PECVD thin films present preferential texturing according to the [004], [112], or [211] directions.

Rutilization of the TiO_2 Thin Films. The transformation of anatase into rutile in powder or bulk TiO_2 materials usually occurs at temperatures around 873−973 K.[26] However, this transformation occurs at much higher temperatures when dealing with thin films.[27,28] Here, we have tried to correlate the temperature of this transformation with other characteristics of the samples. In general, all the thin films kept the anatase structure up to temperatures around 1073−1173 K. Rutilization starts above this temperature and proceeds to a different extent depending on the sample. Figure 9 shows the XRD diagrams of different samples heated at 1073, 1173, 1273, and 1373 K. (P)TiO_2-298 and (P)TiO_2-523 samples behaved in a similar way upon annealing, and only the diagram of the former is included in the figure. In general, complete rutilization occurs at 1373 K. However, while rutilization of IBICVD thin films starts at 1073 K, the transition temperature is ∼1273 K for the PECVD samples [note, however, that for the (P-90Ar)TiO_2 sample the transformation starts already at 1173 K].

Photoelectrochemical Response of the TiO_2 Thin Films. The photoresponse of the different samples has been checked in a photoelectrochemical cell. Figures 10−12 show a series of photocurrent/voltage curves obtained for samples prepared by IBICVD and PECVD under different conditions.

Table 3 summarizes the current values at zero voltage for the different samples. A first point from Figure 10

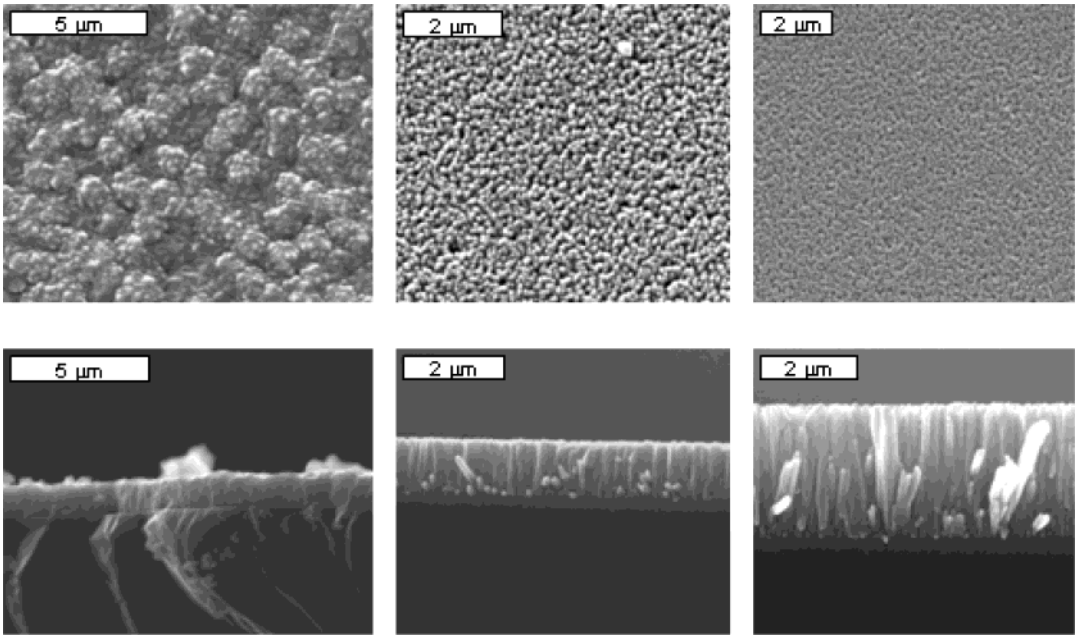

Figure 6. Normal and cross-sectional SEM images of TiO_2 thin films prepared by PECVD: (left) (P-90Ar)TiO_2-523; (middle) (P-85Ar)TiO_2-523; (right) (P-75Ar)TiO_2-523.

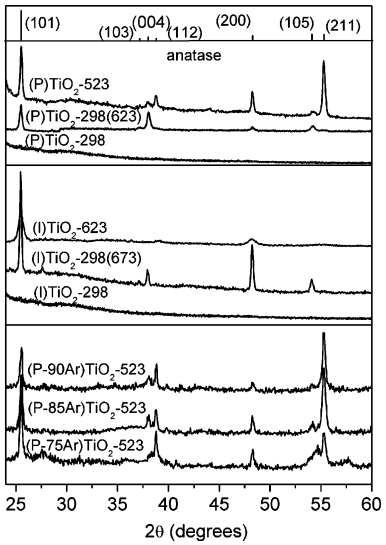

Figure 7. XRD diagrams of TiO_2 thin films prepared according to different protocols: (top) (P)TiO_2-298, (P)TiO_2-298(623), and (P)TiO_2-523 samples; (middle) (I)TiO_2-298, (I)TiO_2-298(673), and (I)TiO_2-623 samples; (bottom) (P-75Ar)TiO_2-523, (P-85Ar)-TiO_2-523, and (P-90Ar)TiO_2-523 samples. The peak intensity profile of randomly oriented anatase is included in the top panel for comparison.

Table 2. Sizes of Crystalline Domains Determined by the Scherrer Method for the Different Samples

sample	crystal size (nm)
(I)TiO_2-298	amorphous
(I)TiO_2-523	amorphous
(I)TiO_2-623	23.5
(I)TiO_2-298(623)	52.8
(P)TiO_2-298	amorphous
(P)TiO_2-523	260.1
(P)TiO_2-298(623)	107.1
(P-75Ar)TiO_2-523	93.5
(P-85Ar)TiO_2-523	96.4
(P-90Ar)TiO_2-523	95.7

that deserves a comment is that the (I)TiO_2-298 sample presents the lowest photocurrent response, although it increases for the (I)TiO_2-523 and (I)TiO_2-623 samples.

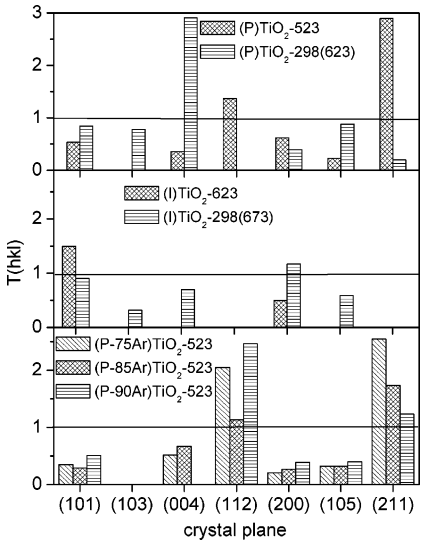

Figure 8. Textural coefficients deduced from the X-ray diagrams reported in Figure 7.

On the other hand, by comparing the photocurrent curves in the three figures it is apparent that the IBICVD samples are less efficient, while those prepared by PECVD, particularly when they are synthesized by heating the substrate at 523 K, depict the maximum photoactivity.

These samples are even more effective than the Degussa P25 reference sample prepared as a photoanode (cf., Figure 11). A general characteristic of the thin films with the highest photoresponse is that they present the anatase structure and have a columnar microstructure with part of the thin film volume occupied by voids and pores (cf., Figures 5 and 6). It is also worthy of mention that the curves in the dark or by selecting the light of the visible spectrum were very similar in all cases, irrespective of the type of samples considered. This means that visible light is not active for the sensitization of the photoanodes.

Discussion

The main objective of this work is to assess the different sample characteristics that favor a high photoresponse of

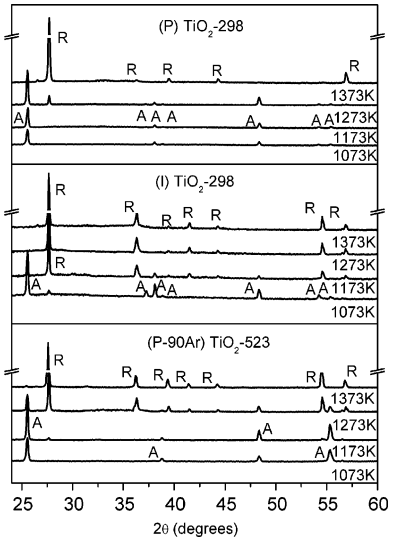

Figure 9. XRD diagrams of the indicated TiO_2 thin films prepared by IBICVD and PECVD and annealed at increasing temperatures between 1073 and 1373 K to induce the anatase−rutile transformation. Typical peaks of the anatase (A) and rutile (R) structures are indicated.

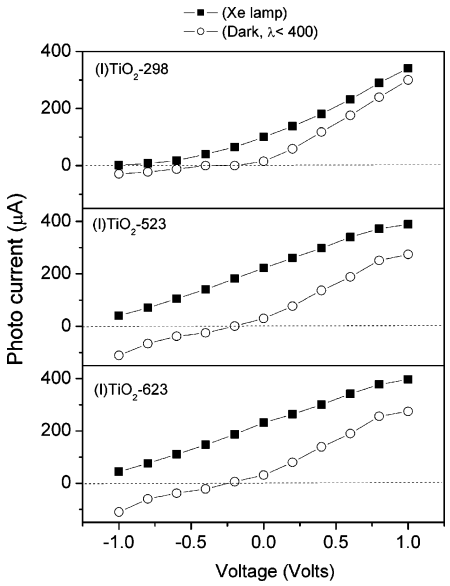

Figure 10. Intensity-versus-voltage curves for TiO_2 thin films prepared by IBICVD acting as photoanodes in a photoelectrochemical cell: (top) (I)TiO_2-298; (middle) (I)TiO_2-523; (bottom) (I)TiO_2-623. Curves are presented for irradiation with the whole spectral range (■) produced by the lamp or by selecting the white light of the spectrum with a filter (○). The dark current coincides with this latter curve.

TiO_2 thin films when used as photoanodes. Another related question is the dependence of the optical properties on the microstructure of the samples.

While analysis relating the photoactivity with the sample characteristics has been carried out with TiO_2 photocatalysts in the powder form,[20−22] equivalent studies with thin films have been less systematic. Possible reasons for this situation are the fact that studies on the photocatalytic behavior of TiO_2 thin films are more recent and that, consequently, there are not well-characterized referencing materials that could be used for comparison. Also, most papers on thin film photocatalysts report one type of preparation procedure, an approach that furnishes few variations in the sample characteristics.

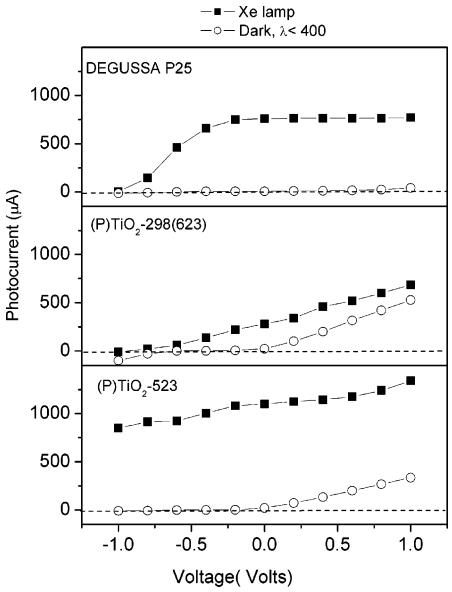

Figure 11. Intensity-versus-voltage curves for TiO_2 thin films prepared by PECVD acting as photoanodes in a photoelectrochemical cell: (top) thin film of Degussa P25 included for comparison; (middle) (P)TiO_2-298(623); (bottom) (P)TiO_2-523. Curves are presented for irradiation with the whole spectral range (■) produced by the lamp or by selecting the white light of the spectrum with a filter (○). The dark current coincides with this latter curve.

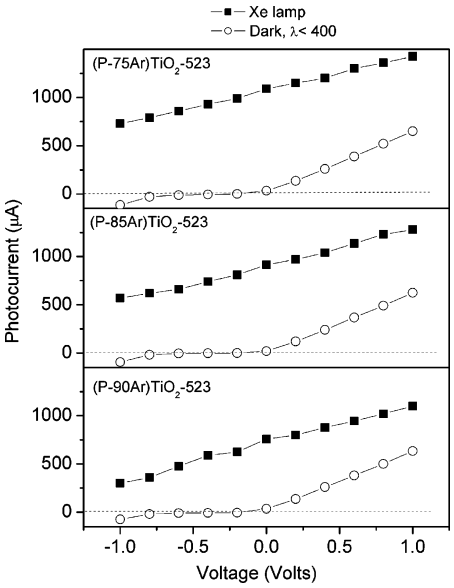

Figure 12. Intensity-versus-voltage curves for TiO_2 thin films prepared by PECVD acting as photoanodes in a photoelectrochemical cell: (top) (P-75Ar)TiO_2-523; (middle) (P-85Ar)-TiO_2-523; (bottom) (P-90Ar)TiO_2-523. Curves are presented for irradiation with the whole spectral range (■) produced by the lamp or by selecting the white light of the spectrum with a filter (○). The dark current coincides with this latter curve.

In the present paper, we have prepared TiO_2 thin films by means of two different preparation methods (i.e., IBICVD and PECVD) according to well-defined preparation protocols. In this way, we have been able to prepare films with large differences in microstructure, crystalline structure, optical properties, and Ti^{3+} concentration centers. The present discussion will be devoted to highlighting the possible correlations existing between the samples characteristics and the optical and photocatalytic behaviors.

Table 3. Current at Zero Voltage for the Different Photoelectrodes

sample	photocurrent (μA)
(I)TiO_2-298	99
(I)TiO_2-523	221
(I)TiO_2-623	233
(I)TiO_2-298(673)	115
(P)TiO_2-298	150
(P)TiO_2-523	1114
(P)TiO_2-298(623)	282
(P-75Ar)TiO_2-523	1083
(P-85Ar)TiO_2-523	913
(P-90Ar)TiO_2-523	759
Degussa P25	766

(a) Optical Properties and Microstructure of TiO_2 Thin Films. Except for the samples with a high concentration of defects, the other thin films were transparent or presented a milky aspect when observed at a grazing angle. The transparent samples, particularly those prepared by IBICVD and PECVD at room temperature, presented a well-defined interference pattern from which the refractive index (n; cf., Table 1) and thickness of the film can be deduced. Similar values of the refractive index were obtained by ellipsometry. From the comparison of the different n values in Table 1, we can deduce that samples prepared by IBICVD are more compact than those obtained by PECVD. This tendency is supported by the fact that in the former case the values approach those reported for bulk TiO_2.[38] Such an assessment of porosity is sustained by the well-described behavior of TiO_2 porous thin films whose experimental refractive index is the average of the refractive indexes of its constituent material(s) and that of the air or the water condensed in the pores.[39]

Table 1 shows that the absorption threshold of the (I)TiO_2-298(673) and (P)TiO_2-523 samples or the (P)TiO_2-298(623) sample presents an apparent shift toward the visible. According to the XRD data (cf., Table 2), these thin films had crystal domains ranging between 50 and 260 nm. Scattering of light at these domains may lead to the damping of the interference pattern of the spectrum (cf., Figures 1 and 2) and to the apparent shift in the absorption threshold.[18,27,28] Reports in the literature about TiO_2 and M/TiO_2 systems (M, a transition metal cation) usually claim a real shift in the absorption threshold toward the visible based on similar observations in the UV−vis spectrum.[40,41] Our results suggest that shifts observed in the UV−vis spectra can be misleading if the films are not sufficiently transparent as a result of light scattering effects.

The SEM analysis of the samples sustains the observed optical behavior of the thin films. Thus, according to the micrographs in Figures 4−6, the (I)TiO_2-298 and (I)TiO_2-523 samples are compact, while the (P)TiO_2-523 sample develops a more open and porous microstructure. As it has been previously discussed, these observations agree with the qualitative assessment on porosity deduced from the value of the refractive indexes.

Particularly interesting is the microstructure of the samples prepared by PECVD at 523 by changing the composition of the plasma gas. These samples have been prepared with the aim of obtaining nonstoichiometric titanium oxide with a high concentration of Ti^{3+} centers that might confer to this sample the capacity to absorb light in the visible region of the spectrum.[18,42] Figure 6 clearly shows the development of a particularly well-defined columnar microstructure for the (P-85Ar)TiO_2-523 and (P-75Ar)TiO_2-523 samples which, according to their UV−vis absorption spectra, are virtually stoichiometric. By contrast, the blue colored (P-90Ar)TiO_2-523 sample must have a high concentration of Ti^{3+} species that would be responsible for the high absorption in the whole UV−vis spectrum. This sample was more globular, although still kept a columnar growth. The development of a well-defined columnar growth for PECVD samples prepared with an Ar-rich plasma gas is an interesting feature deduced from the SEM images of these samples. Although a full understanding of this behavior is outside of the scope of the present paper, the obtained results open a way of tailoring the columnar microstructure of TiO_2 thin films (diameter of columns, separation between columns, etc.) by changing the PECVD deposition conditions.

(b) Thin Film Texture and Crystallinity. The changes in the optical properties and microstructure of the films run parallel with modifications in the crystalline character of the samples. Thus, their structural characterization reveals that, as prepared at room temperature either by IBICVD or by PECVD, the films are amorphous but crystallize into the anatase phase of TiO_2 when annealed in air at $T > 623$ K. After crystallization, differences can be quoted with respect to the size of the crystalline domains and the type of preferential growth of the crystalline planes parallel to the surface of the thin film (i.e., textural crystallization of the films according to certain crystallographic directions, as reported in Figure 8). The data in Table 2 reveal that the size of the crystal domains of the IBICVD samples is smaller than that of the domains developed in the PECVD samples. A well-recognized effect of the ion bombardment on the growth mechanism of thin films is amorphization due to atom displacement and relocation.[24] Similarly, ion bombardment favors the development of a great number of nucleation centers. Both types of effects must contribute to reduce the size of the crystal domains in the (I)TiO_2-623 sample (i.e., 23.5 nm, the smallest size detected among the studied samples). In the (I)TiO_2-298(673) sample, although crystallization is induced by thermal annealing, the size of the crystal domains is still smaller than that in its equivalent (P)TiO_2-298(623). It is likely that the high compactness of the former thin film restricts the mobility and rearrangement displacements of the atomic species, thus limiting the final size of the crystal domains.

PECVD samples prepared at 523 K have crystal sizes $d > 95.0$ nm. In these samples, crystals must develop during the film growth mainly by incorporation of new material to existing nuclei. The fact that the crystal size is smaller in samples prepared with a mixture of $O_2 + Ar$ as the plasma gas while they develop well-defined and thin columns (cf., Figure 6) points to that the columnar growth and the dimension of columns establish restrictions to the size of the crystal domains in this case.

The textural parameters reported in Figure 8 show that, while the IBICVD samples only depict a slight texturing according to the crystallographic directions [101] [i.e., the (I)TiO_2-623] sample and [200] [i.e., the (I)TiO_2-298(673)

(38) Depending on the crystal phase and direction, the refractive index of TiO_2 ranges between 2.481 and 2.609. *Handbook of Chemistry and Physics*, 78th ed.; Lide, D. R., Ed.; CRC Press: New York, 1997.

(39) Alvarez-Herrero, A.; Fort, A. J.; Guerrero, H.; Bernabeu, E. *Thin Solid Films* **1999**, *349*, 212.

(40) Beteille, F.; Morineau, R.; Livage, J.; Nagano, M. *Mater. Res. Bull.* **1997**, *32*, 1109.

(41) Fuerte, A.; Hernández-Alonso, M. D.; Maira, A. J.; Martínez-Arias, A.; Fernández-García, M.; Conesa, J. C.; Soria, J. *Chem. Commun.* **2001**, 2718.

(42) Takeuchi, T.; Nakamura, I.; Matsumoto, O.; Sugihara, S.; Ando, M.; Ihara, T. *Chem. Lett.* **2000**, *12*, 1354.

sample], the PECVD samples show a preferential growth of the (004) planes for the (P)TiO_2-298(623) sample and (211) planes for the (P)TiO_2-523 sample. On the other hand, for the series of samples prepared by PECVD with a mixture of Ar + O_2, the preferential growth of the (211) planes is accompanied by that of the (112) planes. The atom occupancy of these latter planes is smaller than that of the (101) planes, and its development in these samples must be associated with the plasma enhanced method of preparation. It is, therefore, likely that the well-defined columns developed in these samples are aligned along the [211] or [112] crystallographic directions. A comprehensive evaluation of the factors contributing to the preferential growth of the (211) or (112) planes by PECVD at 523 K must consider certain phenomena such as the agglomeration of particles from the gas phase and crystallization induced by heating. In any case, the determination of the photoefficiency of the different samples has shown that the development of a given preferential texture is not a critical factor in determining the photoefficiency of TiO_2 thin films. This result contrasts with the reported higher photoefficiency attributed to TiO_2 powder materials that expose preferentially the (001) and (010) planes at the surface.[43]

(c) Anatase−Rutile Phase Transformation in TiO_2 Thin Films. In this work, we have also studied the anatase−rutile transformation in TiO_2 thin films. This transformation has been reported to occur at 873−973 K for TiO_2 in bulk form,[26] although this temperature may increase depending on factors such as the subdivision degree of the material (i.e., particle size), stabilization of the surface by adsorption of groups such as SO_4^{2-}, PO_4^{3-}, and so forth.[29,30] For thin films, although there are evidences that crystallization occurs at higher temperatures than that for the bulk material,[28,29] the influence of the type of microstructure (i.e., porosity, thickness, columnar growth, etc.) or other parameters, such as crystal size, on the temperature of transformation is not well-proved. Our experiments have shown that transformation into the rutile phase occurs at 1173−1273 K for the PECVD and 1073 K for the IBICVD samples. We think that the higher compactness of the IBICVD samples is a critical factor responsible for this difference.

(d) Relation between Microstructure, Crystalline Structure, and Photoresponse. Whatever the preparation conditions, all the TiO_2 thin films were photoactive when tested in an photoelectrochemical cell under irradiation. However, the photoefficiency was quite different depending on the characteristics of the samples. A first observation is that the original samples prepared at room temperature, either by IBICVD or PECVD, are not very efficient as photoanodes (cf., Table 3). We attribute the poor photoresponse of these samples to their compact and amorphous character. Previous results in the literature have shown that the photoefficiency of amorphous TiO_2 thin films is low and that the photoactivity increases with the crystallinity of samples.[44] Furthermore, many reports have stressed that the most photoefficient crystalline phase of TiO_2 is anatase.[45,46] Therefore, it is not strange that the photoactivity of all the samples increases noticeably when this phase is formed after annealing at $T > 523$ K (cf., Table 3). In general, IBICVD samples annealed in air at $T > 623$ K present a lower photoactivity than those obtained by PECVD. SEM micrographs of IBICVD samples prepared to 523 and 623 K show the formation of well-defined crystallites well-packed in a compact layer where the porosity is small. By contrast, annealed PECVD samples and, particularly, samples prepared by this procedure while heating the substrate at 523 K depict a columnar structure with open pores and voids clearly distinguishable in the SEM micrographs and whose existence is confirmed by the relatively low value of the refractive index of the films (cf., Table 1). We attribute their improved performance toward the photosplitting of water to the higher porosity of these samples. A similar tendency has been found by Xagas et al.[47] showing that the photoefficiency of the TiO_2 thin films increases with the surface roughness associated with a small size of the particles and the development of porosity in the film. The high photoefficiency found for porous thin films would be equivalent to the enhanced photoresponse observed for high-surface-area powders of TiO_2 in aqueous suspensions.[20] However, when the photoresponse of the PECVD samples is compared with that of an electrode made by electrophoretic deposition of the anatase P25 reference material, it is clear that the former type of thin film samples is more efficient for the photosplitting of water (cf., Figure 11 and Table 3). The columnar microstructure of our films would enable a good electrical contact of the titanium oxide crystallites with the titanium plate used as the substrate, and collector of electrons seems to be a reason for this enhanced photoactivity. Other factors, such as an increased surface area due to this microstructure, might also favor a positive photoresponse of the samples. The anatase P25 electrodes are formed by the agglomeration of powder particles, where the poor electrical contact between the grains would be a detrimental factor for the photoefficiency of the system.

The photoelectrochemical behavior of the PECVD samples prepared with a mixture of Ar + O_2 deserves a particular comment. Some of these samples [i.e., (P-75Ar)-TiO_2-523 and (P-85Ar)TiO_2-523] were stoichiometric, and, therefore, no significant differences should be expected with respect to the behavior of the (P)TiO_2-523 sample, as it is actually found (cf., Figures 11 and 12 and Table 3). By contrast, the (P-90Ar) TiO_2 sample was clearly nonstoichiometric and eventual differences in the photoresponse could be expected if the Ti^{3+} centers or continuous bands generated within the titanium oxide structure act as absorption centers leading to a shift of the photoresponse toward the visible.[42,48] Our results with the (P-90Ar)TiO_2-523 sample clearly discard a positive effect of Ti^{3+} doping in favor of the photoactivity of TiO_2 in the visible. The slightly lower photoactivity detected for this sample as compared with the stoichiometric (P)TiO_2-523 agrees with the results of Takeuchi et al.[42] who found a decrease in the photoactivity because of the recombination of e^-−h^+ pairs at the Ti^{3+} centers.

Some papers in the literature have also claimed that sensitization of TiO_2 with carbon deposits embedded in its structure may have a positive influence for this visible sensitization.[49,50] The (P-100Ar)TiO_2-523 sample is formed by a mixture of titanium oxide and carbon and presents no photoactivity. Although more studies should be required to fully characterize the state of carbon in the samples, our preliminary results reveal that carbon plus titanium oxide is not necessarily a requisite for a positive photo-

(43) Martra, G. *Appl. Catal., A* **2000**, *200*, 275.
(44) Yu, J.; Zhao, X.; Zhao, Q. *Thin Solid Films* **2000**, *379*, 7.
(45) Augustynski, J. *Electrochim. Acta* **1993**, *38*, 43.
(46) Ichikawa, Sh.; Doi, R. *Thin Solid Films* **1997**, *292*, 130.
(47) Xagas, A. P.; Androulaki, E.; Hiskia, A.; Falaras, P. *Thin Solid Films* **1999**, *357*, 173.
(48) Takeda, S.; Suzuki, S.; Odaka, H.; Hosano, H. *Thin Solid Films* **2001**, *392*, 338.
(49) Matos, J.; Laine, J.; Herrmann, J. M. *J. Catal.* **2001**, *200*, 10.
(50) Tsumura, T.; Kojitani, N.; Umemura, H.; Toyoda, M.; Inagaki, M. *Appl. Surf. Sci.* **2002**, *196*, 429.

response and that a careful determination of the composition and microstructure should be necessary to ensure photoactivity.

Conclusions

In this paper, we have prepared TiO_2 thin films with different structural and microstructural characteristics to determine the factors that favor the photoactivity of this material when used as a photoelectrode in a photoelectrochemical cell. Thin films have been prepared by IBICVD and PECVD under different deposition conditions. The first method produces very compact films that have a relatively high refractive index. Meanwhile, a rather porous microstructure formed by well-defined columns is obtained by PECVD. These thin films had a lower refractive index because of the partial filling of pores with air or water. In all cases, crystallization into the anatase structure occurs at a temperature around 573 K.

Sample characteristics that enhance photoactivity are the anatase structure of titanium dioxide, a porous microstructure, and the columnar growth. By contrast, the formation of the Ti^{3+} centers incorporated within the structure of nonstoichiometric titanium oxide has no noticeable influence in favoring the photoresponse of this material as a photoanode. The presence of an excess of carbon in the thin film together with titanium oxide has a clear detrimental effect on the photoactivity.

It is also shown that when determining the absorption threshold in TiO_2 thin films by UV−vis absorption spectroscopy, light scattering may occur if the size of the crystal domains is large. This may produce an apparent shift toward the visible in the absorption curve and give the faulty impression that the titanium oxide is active in the visible zone of the spectrum.

Acknowledgment. We thank the EU (Project No. ERK6/CT1999-00015) and the Ministerio de Ciencia y Tecnología of Spain (Project No. MAT2001-2820) for financial support. We thank Dr. T. Girardeau for ellipsometric measurements with some of the samples.

LA034998Y